Gümüşhane University Journal of Science

GUFBD / *GUJS* (2024) 14(4): 1235-1246 doi: 10.17714/gumusfenbil.1534430 Research Article

Field, mineralogical and petrographic features of the Miocene lava around Sağlık and Yatağan area, western Konya/Türkiye

Konya'nın (Türkiye) batısında Sağlık ve Yatağan bölgesindeki Miyosen lavlarının saha, mineralojik ve petrografik özellikleri

Kerim KOÇAK*

Konya Technical University, Engineering&Natural Sci.Faculty, Geological Eng.Department, 42031, Konya

• Received: 16.08.2024 • Accepted: 02.11.2024

Abstract

Extensive lava domes occur west of Konya as a component of subduction-related Neogene Erenlerdağı volcanism. These light grey to grey-coloured domes commonly give rise to topographic elevations and contain some Mafic Microcrystalline Enclaves (MME) with a well-developed chilled zone, up to 4 mm thick. Petrographical and modal image analysis show that the lava samples consist predominantly of plagioclase (andesine, 8-46%, 0.11-4.3 mm), amphibole (3-17%, 0.14-1.613 mm), clinopyroxene (0-14%, 0.035-1.845 mm), biotite (3-12%, 0.09-2.30 mm), epidote (0-8%, 0.078-0.166 mm), piemontite (0-3%, 0.145-0.562 mm), quartz (0-6%, 0.4-2.0 mm), sanidine (0-5%, 0.10-0.17 mm), and opaque iron ore (3-43%), along with accessory minerals apatite and zircon, in various textures, including holocrystalline porphyritic, hypocrystalline porphyritic, glomeroporphyritic, and synneusis. The chilled zone is characterised by phenocrysts of plagioclase (25%) and amphibole (5%) in a holocrystalline porphyritic texture. The amphibole shows opacification and calcitization. The matrix includes plagioclase, amphibole (0.3-0.4 mm), epidote, opaque minerals and rare volcanic glass. The petrographical study suggests that the lava likely experienced mixing or mingling processes during the replenishment of felsic magma by mafic magma, potentially triggering a volcanic eruption. The crystallisation of skeletal and acicular microphenocrysts of plagioclase and acicular apatite indicates rapid crystallisation under undercooled conditions.

Keywords: Image analysis, Konya, Lava, Mineralogy, Miocene, Volcanism

Öz

Konya'nın batısında, dalma-batma ile ilişkili Neojen Erenlerdağı volkanizmasının bir bileşeni olarak geniş lav kubbeleri oluşur. Bu açık gri ila gri renkli domlar yaygın olarak topografik yükseltilere yol açar ve 4 mm kalınlığa kadar iyi gelişmiş bir soğuma zonuna sahip bazı Mafik Mikrokristalin Anklavlar (MME) içerir. Petrografik ve modal görüntü analizi lav örneklerinin çeşitli dokular (holokristalin porfiritik, hipokristalin porfiritik, glomeroporfiritik ve syneusis) içinde başlıca plajiyoklaz (andezin, %8-46), amfibol (%3-17), klinopiroksen (%0-14), biyotit (%3-12), epidot (%0-8), piemontit (%0-3), kuvars (%0-6), sanidin (%0-5) ve opak demir cevheri (%3-43) ile birlikte tali apatit ve zirkondan nimerallerinden oluştuğunu göstermektedir. Soğuma zonu, tam kristalli porfirik bir dokudaki plajiyoklaz (%25) ve amfibol (%5) fenokristalleri ile karakterize edilir. Amfibol, opaklaşma ve kalsitleşme gösterir. Hamur, plajiyoklaz, amfibol (0,3-0,4 mm), epidot ve opak mineralleri içerir. Bu petrografik çalışma, lavın potansiyel olarak bir volkanik patlamayı tetikleyen, muhtemelen felsik magmanın mafik magma tarafından yenilenmesi sırasında fiziksel ve kimyasal karışım süreçlerine uğadığını ileri sürmektedir. İskeletsel ve iğnemsi plajiyoklaz mikrofenokristalinin ve iğnemsi apatitin kristalleşmesi, aşırı soğutulmuş şartlar altındaki hızlı kristalleşmeyi işaret etmektedir.

Anahtar kelimeler: Görüntü analizi, *Konya, lav, mineraloji, Miyosen, volkanizma*

*Kerim KOÇAK; kkocak@ktun.edu.tr

1. Introduction

The Neotectonic phase in Anatolia was characterized by the collision between the Eurasian and Arabian plates, which initiated the westward tectonic movement and led to the formation of major fault systems, such as the East Anatolian and North Anatolian faults (Dewey et al., 1986; Şengör et al., 1985). This tectonic activity was accompanied by widespread volcanic activity, covering an area of approximately 85,000 km² in central and western Anatolia (Blumenthal, 1944), with notable calc-alkaline volcanic products near Konya (Figure 1).

Blumenthal (1944) and Üstündağ (1987) explored the geological features of the region, identifying Tertiary rocks, proposing a geological map with an Ordovician metamorphic basement, and suggesting a tectonic phase between the Paleozoic and Mesozoic in the Konya and Aksehir areas. Additional research by Eren (1993), Hekimbaşı (1996), Özcan et al. (1988) and Uyanık and Koçak (2016) identified the "Bozdağ formation" in a Pre-Triassic region and detailed the stratigraphic units in the Karadag area. Keller et al. (1977) mapped Neogene volcanism at NW Konya and dated volcanic, while Temel et al. (1998) linked calc-alkaline volcanic activity in Konya to the subduction of the African plate during the Middle to Late Miocene. Karakaş and Kadir (2000) recognised crystallisation patterns, while Kurt et al. (2003) proposed that the volcanics originated from subduction processes. Kurt et al. (2005) investigated the Erenler-Alacadağ volcanics, which are characterised by an andesite-dacite composition with subalkaline properties and proposed that these rocks originated from continental crust as a result of old subduction-related volcanic activity. Karakaya (2009) discussed the impacts of hydrothermal alteration, highlighting significant enrichment in rocks undergoing kaolinitic and alunitic changes. Kocak and Zedef (2016a) analyzed the geochemical properties of lava and its mafic enclaves, suggesting that the enclaves may have formed from the hybridization of mafic magma with partially crystallized felsic magma. Uyanık and Koçak (2016) and Kocak and Zedef (2016b) examined the Neogene Erenlerdağı volcanism, proposing that the volcanic formations likely resulted from Assimilation-Fractional Crystallization (AFC) and/or magma mixing processes. Koçak (2023) outlines the main petrographical features of the lava with restricted thin sections.

Volcanic events in this area took place from 13.72 to 3.35 million years ago (Asan & Erturk, 2013; Keller et al., 1977), with lava dome formations dating between 10.9 and 3.35 million years. According to Keller et al. (1977) the most ancient lava domes of the Erenlerdağı Alacadağ volcanic region, situated to the north of Hacibabadağ in the northwest part of the study area, date back to 10.55–10.9 million years ago. Lava domes in the Konya volcanic field's western segment, namely, in the Mesutlar, Fasillar, Huseyinler, Gevrekli, and Bostandere regions, represent the study area's most recent volcanic features. These domes intrude into Upper Pliocene continental limestone and carbonaceous marl. Radiometric dating indicates that the Fasillar lava domes are approximately 3.2 million years old, while the Gevrekli lava domes date to around 3.35 million years. That is, in the region, there is ageing in lava from south to north, so it is considered that the lava in the study area, which is relatively farther north, could be older (Miocene). The geological structure of the study region features a varied Pre-Miocene foundation consisting of metamorphic, ophiolitic, and marine deposits, along with Upper Miocene-Pliocene lake-fluvial sediments, volcanic materials, and Quaternary layers (Figure 1).

Located east of Sağlık town and west of Yatağan in western Konya, the study area features two rock quarries providing insights into the relations between Neogene lava and its MME. The light grey to grey lavas often create elevated topographical features, with a noticeable joint system. (Figure 2). It is characterised by the existence of MME (Figure 2 b), indicating mingling in the felsic magma. The MME is finer-grained than its host, ranges in size from a few centimetres to meters and shapes from ellipse/rounded-angular. A well-developed chilly zone forms between the lava and enclave, up to 4 mm but mostly 1.25-2.5 mm in thickness. It is aimed to characterize the field, geological, and petrographical properties of the Miocene lava and its associated chilled zones in detail, as well as determine the mineral sizes and modal mineralogical composition using "Kameram" software.

2. Material and methods

Approximately 100 samples were collected and from 70 of which, thin sections were made. Their mineralogical and petrographical characteristics were examined using a polarizing microscope at the Department of Geological Engineering, Konya Technical University. An image analysis software called

“Kameram” is used for modal analysis and measuring the size of the minerals and reaction rims around biotite and opaque iron ore.

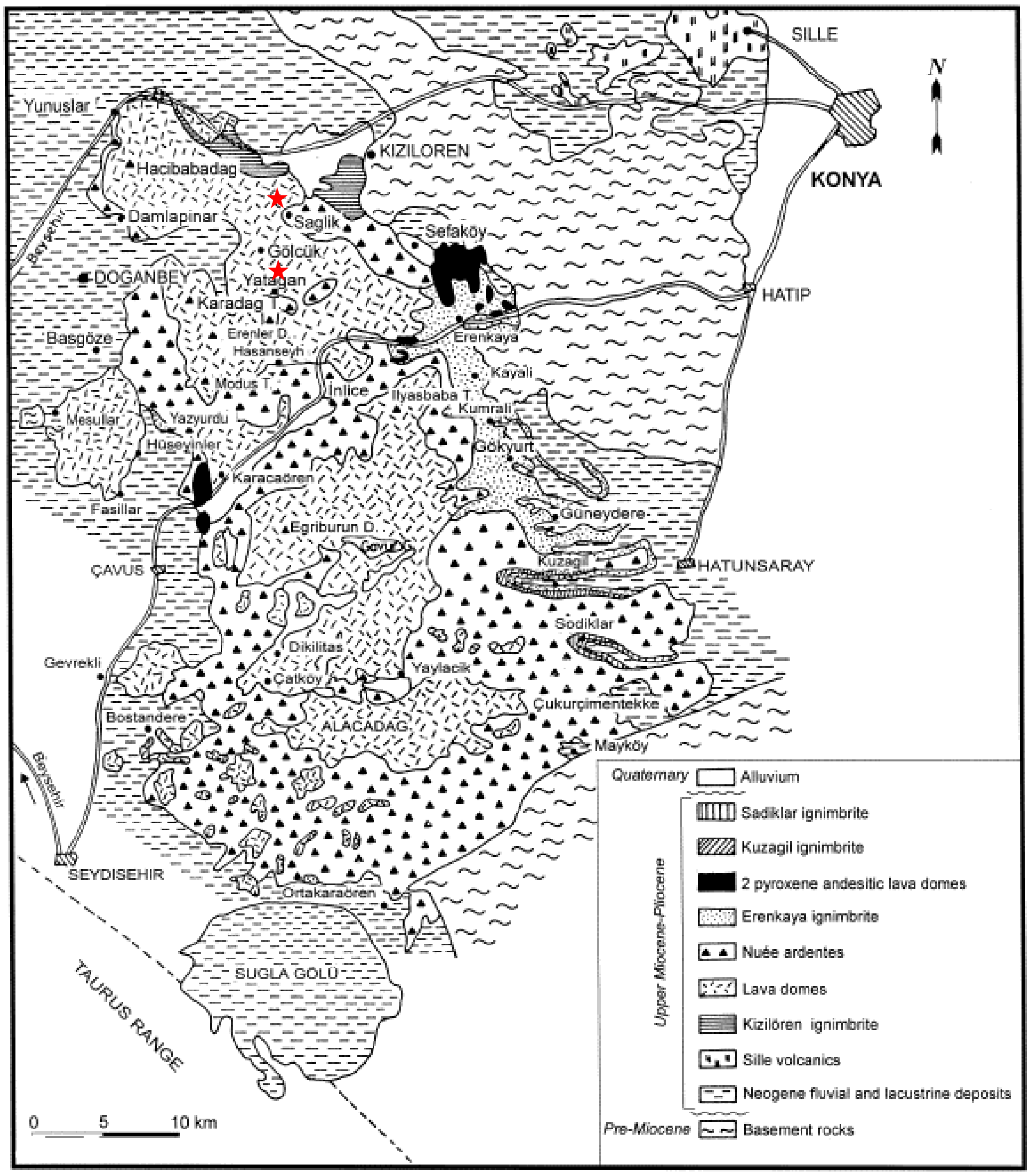

Figure 1. Location and geological maps of the study area (Keller et al., 1977). ★: Rock quarries studied.

Figure 2. Lava dome (a) and enclave with well-developed chilly zone (b).

3. Petrography

3.1. Lava

As main constituents, the samples contain plagioclase (8-46%, 0.11-4.3 mm), amphibole (3-17%, 0.14-1.613 mm), clinopyroxene (0-14%, 0.035-1.845 mm), biotite (3-12%, 0.09-2.30 mm, Figure 3, Figure 4,), epidote (0-8%, 0.078-0.166 mm), piemontite (0-3%, 0.145-0.562 mm), quartz (0-6%, 0.4-2.0 mm), sanidine (0-5%, 0.10-0.17 mm), and opaque iron ore (3-43%, 0.084-0.503mm), with apatite and zircon as accessory phase. The samples have a holocrystalline porphyric and hypocrystalline porphyric texture with PI (Porphyritic Index=area of phenocrysts over the total area of the thin section x 100) up to 33, and synneusis, texture. They also display mostly monomineralic (plagioclase) (Figure 3a) and rare polymineralic (plagioclase and opaque iron ore) glomeroporphyritic textures, which occur in closed configurations with embedded component contacts. The ground mass microlites are mostly tabular to prismatic, and minor acicular. Common alteration types include sericitisation, saussuritization and calcitization.

The plagioclase crystal is predominantly subhedral exhibiting acicular and skeletal texture (0,44-0,957 mm). It also shows fine-sieve (Figure 3b-d) texture, which may occur as a core (0.637-0.905 mm), a rim (0.012-0.299 mm), or an inner rim (0.066-0.104 mm) between the core and rim. However, these features are mostly present at the periphery but absent from the central region. The closely packed and high-density arrangement (total area/number of inclusions) results in a dusty appearance. It is characterised by various twinning types, including simple albite, Carlsbad, albite-pericline, and patchy (Figure 3b-e), with rare flame twinning. It forms commonly as tabular, and rarely acicular crystals.

The crystal displays typical oscillatory zoning (OZ), with the core possibly containing some inclusions. The contact rim is generally straight but can be resorbed (Figure 3f). Resorption is common and observed in multiple forms, such as resorbed crystal habits (external resorption) and resorption boundaries within the plagioclase crystals (internal resorption). The plagioclase has an andesine composition (An_{45}), as determined in the crystals showing albite twins with uniform illumination when (010) is parallel to N-S crosshairs by the Michael Levy method (Kerr, 1959). The amphiboles may record various stages of progressive alteration; a dark reaction rim (Figure 4a) is common in the amphiboles (0.23-3.0 mm). In the advanced stage of alteration, they may form hexagonal pseudomorph crystals (0.5 mm) that are yellowish, reddish, and blackish brown and typically contain plagioclase as an inclusion, with some albite twinning. Intense alterations may have transformed the amphibole into an aggregate of opaque iron ore, chlorite, and epidote (0.6 mm). The brownish biotite is subhedral (Figure 4b) and mostly replaced to amphiboles. It contains plagioclase (0.023-0.117 mm) and zircon as inclusions. The biotite is surrounded by a reaction rim (width: 0.28-0.330 mm) that includes plagioclase (0.147-0.244 mm) with patchy twinning and sieve texture, epidote (0.048-0.099 mm), quartz crystals (0.09-0.16 mm), and opaque iron ore (0.081-0.197 mm).

The subhedral to anhedral clinopyroxene (Figure 4c) is subordinate with slight pleochroism in the shades of light green. It has commonly opaque iron crystallisations (0.09 mm as a diameter) ore at its core (1.2 mm). The quartz is predominantly subhedral to anhedral but can also be euhedral and embayed (Figure 4d). Anhedral quartz is sometimes rimmed by epidote (0.083 mm), forming "ocelli quartz" (Figure 4e). The sanidine is characterised by Carlsbad twinning. Epidote is mostly subhedral and shows bright birefrigence colour. It is mostly developed in and around clinopyroxene. The piemontite is subhedral to anhedral and characterised by having typical reddish brown to red colour. The apatite is noted for its characteristic needle shape (Figure 4f), while zircon is distinguished by its very high relief. The matrix includes plagioclase, pyroxene (0.058-0.172 mm), epidote, opaque iron ore (0.189 mm), and rare volcanic glass. The plagioclase microliths vary in length from 0.053 to 0.167 mm, with an average length of 0.102 mm.

3.2. Chilly zone

The lava has a transitional contact with MMEs, which may be crossed by vesicles (Figure 5). The microscopic studies indicate that the chilly zone consists mainly of plagioclase (0.4-1.2 mm, 25%) and amphibole (5%) as phenocrystals (PI: 30%, Figure 6). The amphibole exhibits opacification and calcitization. The matrix consists of plagioclase, amphibole (0.3-0.4 mm), epidote (0.138 mm) and opaque minerals in a holocrystalline porphyric texture. The modal analysis by Kameram software shows that the host lava has less ferromagnesian (biotite, amphibole) and opaque mineral than its MME (Figure 5b, Figure 6).

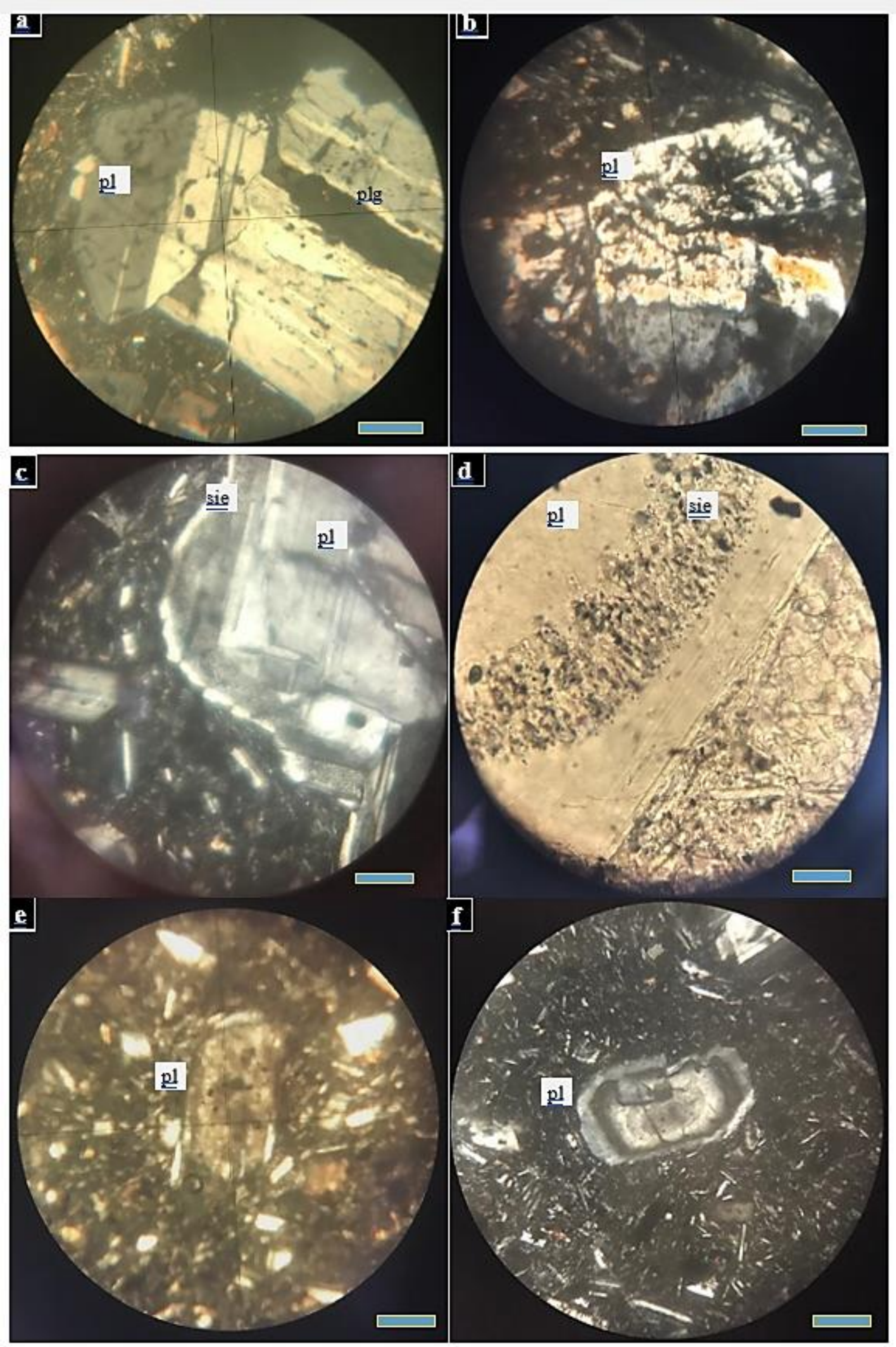

Figure 3. Represented photomicrograph of the plagioclases; cross-polarized (a-c, e-f), and light plane-polarized light (d). Scale bar is 0,2 mm (a,f), 0.1 mm(e-f). pl: plagioclase, sie: sieve texture. a) plagioclase with albite-carlsbad twinning and glomeroporphyritic texture, b) Skeletal plagioclase, c) plagioclase with sieve texture, d) Close up of sieve texture in plagioclase, e) Plagioclase showing patchy twinning, f) Internally and externally resorbed plagioclase with oscillatory zoning.

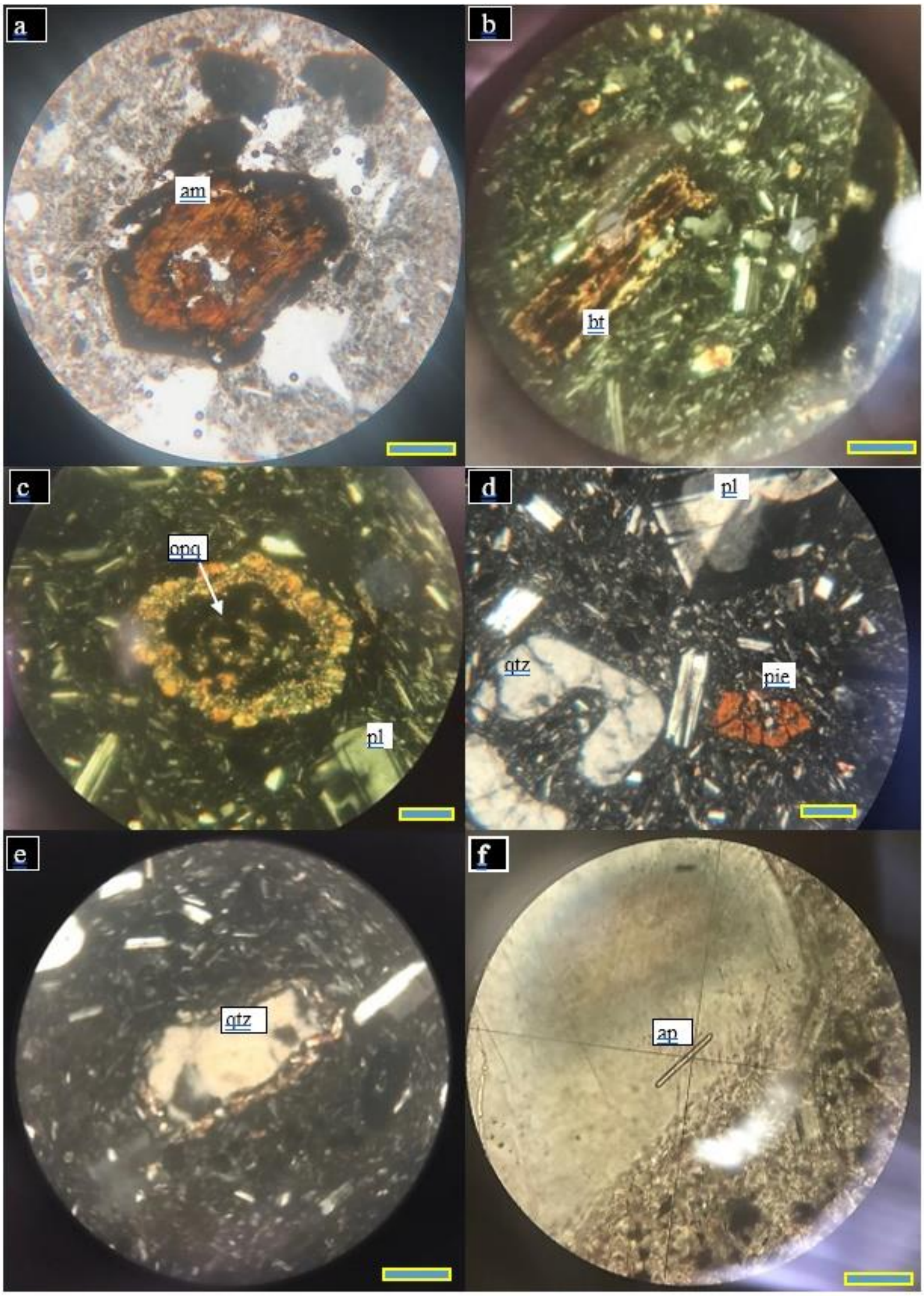

Figure 4. Represented photomicrographs of the samples; cross-polarized (b-e), light plane-polarized light (a,f). Scale bar is 0,2 mm (a- e), 0.1 mm(f). px: clinopyroxene, am: amphibole, pl: plagioclase, sn: sanidine, qtz: quartz, pie: piemontite, ap: apatite, opq: opaque iron ore. a) Brown amphibole rimmed by opaque iron ore, b) chloritised biotites are rimmed by plagioclase and epidote, c) clinopyroxene pseudomorph. d) Resorbed quartz and piemontite, e) Ocelli quartz rimmed by epidote, f) Zoned plagioclase with needle-shaped apatite.

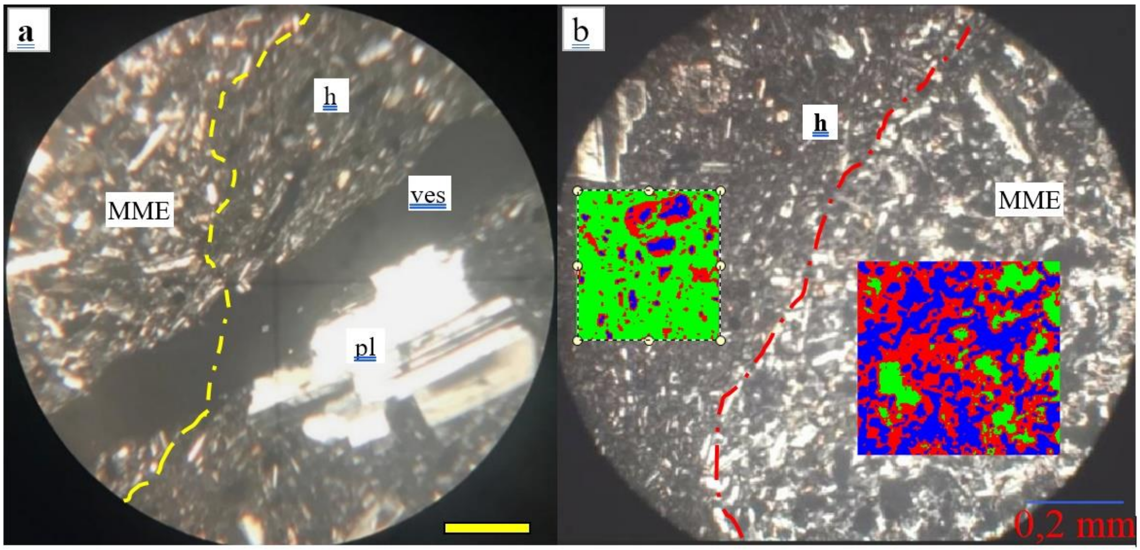

Figure 5. a) Contact between MME and its host, crossed by vesicle(ves). XN, Scale bar is 0.2 mm. **b)** modal analysis of lava (h) and its MME; pl: plagioclase, Red: biotite, amphibole; Blue: feldspars and, quartz; Green matrix

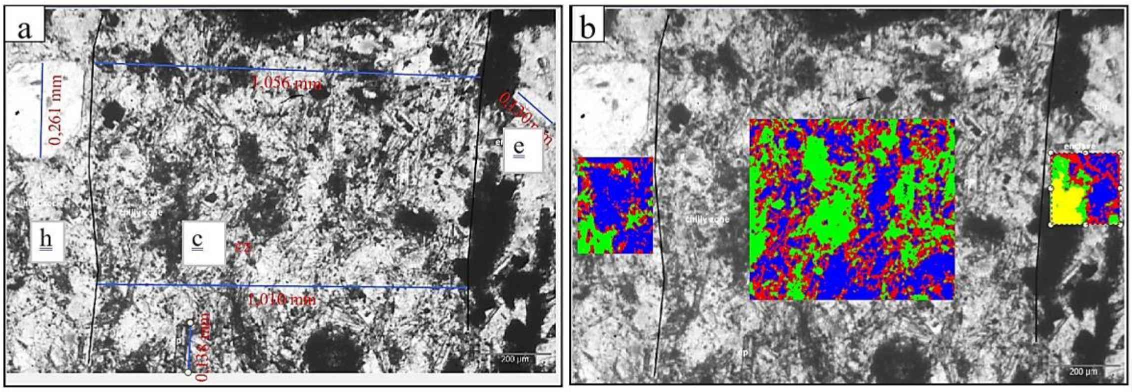

Figure 6. a) Lava and MMEs with a dark-coloured chilly zone, and **(b)** its modal analysis. Chilly zone (c), enclave (e), host (h). Red: biotite, amphibole; Blue: feldspars, quartz; Green matrix, Yellow: opaque iron ore.

4. Discussions

The petrographic study reveals that the lava samples are composed of plagioclase (andesine, 8-46%, 0.11-4.3 mm), amphibole (3-17%, 0.14-1.613 mm), clinopyroxene (0-14%, 0.035-1.845 mm), biotite (3-12%, 0.09-2.30 mm), epidote (0-8%, 0.078-0.166 mm), piemontite (0-3%, 0.145-0.562 mm), quartz (0-6%, 0.4-2.0 mm), sanidine (0-5%, 0.10-0.17 mm), and opaque iron ore (3-43%), and accessory apatite and zircon in various texture, namely, holocrystalline porphyric, hypocrystalline porphyric and glomeroporphyritic texture. It also shows synneusis texture, which refers to the phenomenon where crystals in magma with a high liquid content coalesce and adhere to one another (Schwindinger, 1999). This process typically requires mechanisms such as shear flow or turbulent mixing to align the crystals, although it can also occur during the passive settling of crystals within a liquid medium (Schwindinger, 1999). The lack of chilly zone in the plagioclase with synneusis texture, suggests that the crystals were rarely in motion during their formation, which might be attributed to the dynamically active convection or turbulence within the crystallising magma. Thus, the synneusis texture is likely to be formed by shear flow.

Sieve-textured plagioclase phenocrysts and glomerocrysts (Figs 5a, b and 7a) are common within the lava samples. The sieve texture is characterised by small, interconnected inclusions of glass or other matrix material, giving the crystal a porous look (Tsuchiyama, 1985). Experimental studies suggest that these textures can be produced by through heating (Johannes et al., 1994) rapid decompression (Nelson & Montana, 1992) and chemical disequilibrium (Tsuchiyama, 1985) which may be linked to processes like magma replenishment. Alternatively, the presence of sieve-textured plagioclase crystals and glomerocrysts might reflect initial crystal-liquid interactions between the host magma and the enclave-forming magma before rapid cooling (Eichelberger, 1980). The fine-sieve texture in the samples also displays slight resorption characteristics, such as curved zone boundaries (Figure 3d), suggesting minor dissolution processes occurred during their formation (Ginibre et al., 2002). The varying thickness of the sieve-textured zones is likely related to the extent of disequilibrium experienced by the crystals.

The plagioclase shows OZ, which frequently develops as a characteristic pattern resulting from comparatively gradual crystallisation processes in crystals (Muncill & Lasaga, 1987). It indicates a growth history within a liquid medium by retaining earlier euhedral forms that develop as the crystal expands (Vernon, 2010). The fine OZ domain in the samples shows slight resorption characteristics such as curved zone corners (Figure 3d), suggesting slight dissolution occurred during their development (Ginibre et al., 2002).

The plagioclase displays patchy zoning, likely resulting from the dissolution of the crystal core due to decompression followed by feldspar crystallisation adapting to the altered conditions (Vernon, 2004). Additionally, this zoning may arise from interactions between two compositionally distinct magmatic systems, such as felsic and mafic magmas (L'Heureux & Fowler, 1994), or increased H_2O levels during plagioclase crystallisation (Cao et al., 2019). The patchy zoning typified by amoeboid patches, exhibits a certain level of crystallographic orientation along the cleavage planes. It is commonly linked to two distinct processes: (1) resorption followed by overgrowth (Ginibre & Wörner, 2007), and (2) skeletal growth with subsequent infilling (Shibata, 1990). The patchy zoning with irregular amoeboid patches is interpreted (Bennett et al., 2019) to be formed as a consequence of crystal resorption either along cleavage planes leading to crystallographic alignment and elongation of patches or occurring randomly throughout the crystal structure.

Opacitic rims frequently occur in hydrated minerals like biotite and amphiboles within volcanic rocks. The amphibole exhibits a common reaction rim, which results from various conditions, such as increased temperatures, progressive magma ascent and decompression, and decreased water content and oxygen fugacity within the melt (Ridolfi et al., 2008). The reaction rim is classified as 'black' and 'gabbroic' types, based on whether plagioclase is present in the rim (Garcia & Jacobson, 1979). The amphibole in lava samples has both black and gabbroic-type rims. Garcia & Jacobson (1979) attributed the formation of the gabbroic type to a reduction in fH_2O within the magma reservoir, while the black type was linked to oxidation and dehydrogenation processes during or after extrusion. That is, the reaction rim is probably formed by a reduction in fH_2O within the magma reservoir during or after extrusion. The amphiboles, exhibiting rims ranging from 30 to 60 mm and characterised by a pronounced histogram peak around 48 micrometres, likely experienced extended periods outside the stability field of amphiboles. The amphibole reaction rims could have been developed by the intrusion of fresh magma, represented by the presence of MMEs, into the pre-eruption magma chamber.

In an experimental study, Feeley & Sharp (1996) propose that the conversion of biotite phenocrysts into anhydrous minerals, such as plagioclase and magnetite, as a rim, indicates an increase in thermal conditions or a rejuvenation of magma chambers. The decomposition of biotite crystals and the formation of reaction rims are suggested to be influenced by the bulk composition and temperature of the surrounding lava, as well as the water content within the biotite crystals.

The sample also exhibits ocelli quartz. Vernon (1991) suggests that during the mixing of mafic and felsic magmas, quartz crystals from the felsic magma are introduced into a new, more mafic hybrid environment, where they become unstable. The marginal dissolution of quartz xenocrysts extracts latent heat of crystallisation from the adjacent melt, leading to localized undercooling. This undercooling promotes the nucleation of mafic minerals, forming fine-grained aggregates around the quartz xenocrysts. Subsequent quartz precipitation may 'lock in' the mafic mineral rim, preserving the texture and resulting in an outer rim devoid of mafic minerals. A comprehensive review by Palivcova et al. (1995) on the ocellar texture and its petrogenetic interpretations concluded that magma mixing is the only process that satisfactorily explains its occurrence.

The samples contain minerals from the epidote group, including epidote and piemontite. The pink-coloured mineral in the samples is identified as piemontite; tough detailed microchemical analysis Katerinopoulou et al. (2014) reveals that the minerals with a distinctive red to pink hue are Mn-bearing epidote and Mn-bearing clinozoisite. The composition of the epidote, particularly its Fe^{3+} content, is significantly influenced by oxygen fugacity. Higher oxygen fugacity levels stabilize Fe-rich epidote variants while reducing conditions near the quartz-fayalite-magnetite equilibrium favour the formation of Al-rich epidote. It is experimentally shown that high oxygen fugacity is essential for stabilizing piemontite. Factors such as hydrothermal buffering and pre-existing minerals that sustain high oxygen levels contribute to this stability (Keskinen & Liou, 1987). Thus, it is likely that Fe-rich epidote and piemontite might have been formed in high oxygen fugacity environments by hydrothermal processes.

The microcrystals in the groundmass predominantly exhibit tabular to prismatic forms, with a lesser occurrence of acicular shapes. It is experimentally shown that the crystal morphology transitions from euhedral tabular forms to spherulitic structures, passing through prismatic, hopper, skeletal, and dendritic habits with an increase in the degree of undercooling (Suzuki & Fujii, 2010). The presence of tabular and prismatic microlites in the samples suggests that their formation occurred under conditions of minimal undercooling.

Chilled margins (Figure 5, Figure 6) suggest that the MMEs represent part of a larger enclave that disaggregated in a semi-ductile state during entrainment in the host magma.

In sum, the lava with MMEs, might have undergone mixing/mingling processes during replenishment by a mafic magma of a felsic magma possibly triggering a volcanic eruption, as evidenced by the development of sieve texture, amphibole reaction rims, ocelli quartz and acicular apatite. The intrusion of denser basalt into a lighter reservoir is capable of generating viscous gravity currents that spread along the floor. The shear flow indicated by the synneusis texture, can reduce melt viscosity and facilitate mixing. Forcible mafic intrusion into a felsic magma chamber can induce fountaining, which correlates with increased local shear rates (Campbell & Turner, 1986). Fluid dynamical analyses and observational data (e.g. Bacon, 1986) indicate that in calc-alkaline reservoirs, mixing and mingling is most likely initiated by boundary layer instabilities (J. Eichelberger, 1980) at a centimetre to decimetre wavelength scale (Bacon, 1986) or by the disintegration of injected magma dykes (Hodge et al., 2012), which is the case in the study area. The quenching process is characterised by skeletal and acicular microphenocrysts of plagioclase (Lofgren, 1974) and acicular apatite (Wyllie et al., 1962), which suggest rapid crystallisation under undercooled conditions (Bacon, 1986).

5. Conclusions

The mineralogical and petrographical characteristics, along with the modal composition, have been determined for the samples. Evidence of mixing or mingling, resulting from the intrusion of mafic magma into a pre-eruption magma chamber, is suggested by the presence of fine-sieve texture, patchy zoning, reaction rims on amphibole, ocelli quartz, skeletal and acicular microphenocrysts of plagioclase, and acicular apatite. During the ascent of magma, tabular and prismatic microlites likely formed by adiabatic decompression. The lava samples also underwent hydrothermal alteration in an environment with high oxygen fugacity, leading to the development of Fe-rich epidote and piemontite

Acknowledgements

I express my gratitude to the reviewers, Salim Oncel and Bahattin Güllü, for their valuable insights and constructive feedback, which significantly enhanced the quality of this manuscript. Thanks also to Selcuk and Konya Technical Universities for financial and logical support.

Declaration of ethical code

Author follows all ethical guidelines including authorship, citation, data reporting, and publishing original research. The author of this article declare that the materials and methods used in this study do not require ethics committee approval and/or legal-special permission.

Conflicts of interest

The author declares that there is no conflict of interest.

References

Asan, K., & Erturk, M. A. (2013). First Evidence of Lamprophyric Magmatism from the Konya Region, Turkey: a Genetic Link to High-K Volcanism. *Acta Geologica Sinica-English Edition*, *87*(6), 1617-1629. https://doi.org/10.1111/1755-6724.12163

Bacon, C. R. (1986). Magmatic Inclusions in Silicic and Intermediate Volcanic-Rocks. *Journal of Geophysical Research-Solid Earth and Planets*, *91*(B6), 6091-6112. <Go to ISI>://WOS:A1986C311900014

Bennett, E. N., Lissenberg, C. J., & Cashman, K. V. (2019). The significance of plagioclase textures in mid-ocean ridge basalt (Gakkel Ridge, Arctic Ocean). *Contributions to Mineralogy and Petrology*, *174*(6). https://doi.org/10.1007/s00410-019-1587-1

Blumenthal, M. M. (1944). Bozkır Güneyinde Toros Dağlarının Serisi ve Yapısı. *İst.Üniv. Fen Fak. Mec*(B), 30.

Campbell, I. H., & Turner, J. S. (1986). The influence of viscosity on fountains in magma chambers. *Journal of Petrology*, *27*(1), 1-30.

Cao, M., Evans, N. J., Reddy, S. M., Fougerouse, D., Hollings, P., Saxey, D. W., McInnes, B. I. A., Cooke, D. R., McDonald, B. J., & Qin, K. (2019). Micro- and nano-scale textural and compositional zonation in plagioclase at the Black Mountain porphyry Cu deposit: Implications for magmatic processes. *American Mineralogist*, *104*(3), 391-402. https://doi.org/10.2138/am-2019-6609

Dewey, J., Hempton, M., Kidd, W., Saroglu, F., & Şengör, A. (1986). Shortening of continental lithosphere: the neotectonics of Eastern Anatolia—a young collision zone. *Geological Society, London, Special Publications*, *19*(1), 1-36.

Eichelberger, J. (1980). Vesiculation of mafic magma during replenishment of silicic magma reservoirs. *Nature*, *288*(5790), 446-450.

Eichelberger, J. C. (1980). Vesiculation of mafic magma during replenishment of silicic magma reservoirs. *Nature*, *288*(5790), 446-450. https://doi.org/10.1038/288446a0

Eren, Y. (1993). Konya kuzeybatısında Bozdağlar Masifinin otokton ve örtü birimlerinin stratigrafisi (in Turkish). *Geol Bull Turk*, *36*, 7-23.

Feeley, T. C., & Sharp, Z. D. (1996). Chemical and hydrogen isotope evidence for in situ dehydrogenation of biotite in silicic magma chambers. *Geology*, *24*(11), 1021-1024. https://doi.org/10.1130/0091-7613(1996)024<1021:Cahief>2.3.Co;2

Garcia, M. O., & Jacobson, S. S. (1979). Crystal clots, amphibole fractionation and the evolution of calc-alkaline magmas. *Contributions to Mineralogy and Petrology*, *69*(4), 319-327. https://doi.org/10.1007/BF00372257

Ginibre, C., & Wörner, G. (2007). Variable parent magmas and recharge regimes of the Parinacota magma system (N. Chile) revealed by Fe, Mg and Sr zoning in plagioclase. *Lithos*, *98*(1-4), 118-140.

Ginibre, C., Kronz, A., & WoÈrner, G. (2002). High-resolution quantitative imaging of plagioclase composition using accumulated backscattered electron images: new constraints on oscillatory zoning. *Contributions to Mineralogy and Petrology*, *142*(4), 436-448.

Hekimbaşı, E. B. (1996). *Petrology and geochemistry of Ladik-KurşunluSızma-Yükselen (Konya) Region* Selcuk University]. Konya.

Hodge, K. F., Carazzo, G., & Jellinek, A. M. (2012). Experimental constraints on the deformation and breakup of injected magma. *Earth and Planetary Science Letters*, *325*, 52-62.

Johannes, W., Koepke, J., & Behrens, H. (1994). Partial melting reactions of plagioclases and plagioclase-bearing systems. *Feldspars and their reactions*, 161-194.

Karakaş, Z., & Kadir, S. (2000). Devitrification of Volcanic Glasses in Konya Volcanic Units, Turkey. *TJES*.

Karakaya, N. (2009). REE and HFS element behaviour in the alteration facies of the Erenler Dagi Volcanics (Konya, Turkey) and kaolinite occurrence. *Journal of Geochemical Exploration*, *101*(2), 185-208. https://doi.org/10.1016/j.gexplo.2008.07.001

Katerinopoulou, A., Balic-Zunic, T., Kolb, J., Berger, A., & Secher, K. (2014). Manganiferous minerals of the epidote group from the Archaean basement of West Greenland. *Bulletin of the Geological Society of Denmark, 62,* 27-37. <Go to ISI>://WOS:000346602400002

Keller, J., Jung, D., Burgath, K., & Wolff, F. (1977). Geologie und petrologie des Neogenen kalkalkali- vulkanismus von Konya (Erenler Dağ - Alaca Dağ - Massiv. *Geologisches Jahrbuch Hessen, 25,* 37-117.

Kerr, P. (1959). Optical Mineralogy. In: McGraw-Hill Book Company, Inc.

Keskinen, M., & Liou, J. (1987). Stability relations of Mn–Fe–Al piemontite. *Journal of Metamorphic Geology*, *5*(4), 495-507.

Koçak, K. (2016). Geochemical characteristics of the mafic enclaves and their hosts from Neogene Erenlerdagı volcanites, around Yatagan village and Sağlık town (Konya), central Turkey. 14th Intern. Congress, Thessaloniki, May 2016, Thessaloniki.

Koçak, K. (2023). Petrographic characteristics of the Neogene lava dome around Sağlık and Yatağan area, Konya/Türkiye. 2nd International Karatekin Science And Technology Conference, Çankırı, Türkiye.

Kocak, K., & Zedef, V. (2016a). Geochemical Characterisics Of The Lava Domes in Yatagan Village And Sağlık Town, From Erenlerdagı (Konya, Central Turkey) Volcanites. Acta Geobalcanica, 2(1), 7-19.

Kocak, K., & Zedef, V. (2016b). Geochemical characteristics of the lava domes in Yatagan village and Sağlik town, from Erenlerdagi (Konya, Central Turkey) volcanites. Acta Geobalcanica| Volume, 2(1), 7-19.

Kurt, H., Özkan, A. M., & Kocak, K. (2003). Geology, Petrography And Geochemistry Of The Subduction Related Volcanic Rocks, West Of Konya, Central Anatolia. *Türkiye Jeoloji Bülteni*, *46*(2), 39 – 51

Kurt, S., Akgül, B., & Kurt, H. (2005). Sağlık-Erenkaya (Konya batısı) yöresi volkanik kayaçlarının petrografik ve jeokimyasal özellikleri. *Fırat Üniversitesi Fen ve Mühendislik Bilimleri Dergisi*, *17*(1), 190 - 204.

L'Heureux, I., & Fowler, A. D. (1994). A nonlinear dynamical model of oscillatory zoning in plagioclase [Article]. *American Mineralogist*, *79*(9-10), 885-891.

Lofgren, G. (1974). An experimental study of plagioclase crystal morphology; isothermal crystallization. *American Journal of Science*, *274*(3), 243-273.

Muncill, G. E., & Lasaga, A. C. (1987). Crystal-growth kinetics of plagioclase in igneous systems; one-atmosphere experiments and application of a simplified growth model. *American Mineralogist*, *72*(3-4), 299-311.

Nelson, S. T., & Montana, A. (1992). Sieve-textured plagioclase in volcanic rocks produced by rapid decompression. *American Mineralogist*, *77*(11-12), 1242-1249.

Özcan, A., Göncüoğlu, M. C., Turhan, N., Uysal, S., & Şentürk, K. (1988). Late Palaeozoic evolution of the Kütahya-Bolkardağ Belt. *METU Journal of Pure and Applied Science*, *21,* 211-220.

Palivcova, M., Waldhausrova, J., & Ledvinkova, V. (1995). Ocelli in mafic rocks of granitic complexes. *Krystalinikum, 22,* 149-186.

Ridolfi, F., Puerini, M., Renzulli, A., Menna, M., & Toulkeridis, T. (2008). The magmatic feeding system of El Reventador volcano (Sub-Andean zone, Ecuador) constrained by texture, mineralogy and thermobarometry of the 2002 erupted products. *Journal of Volcanology and Geothermal Research*, *176*(1), 94-106. https://doi.org/10.1016/j.jvolgeores.2008.03.003

Schwindinger, K. R. (1999). Particle dynamics and aggregation of crystals in a magma chamber with application to Kilauea Iki olivines. *Journal of Volcanology and Geothermal Research*, *88*(4), 209-238.

Şengör, A. M. C., Görür, N., Şaroğlu, F., Biddle, K. T., & Christie-Blick, N. (1985). Strike-Slip Faulting and Related Basin Formation in Zones of Tectonic Escape: Turkey as a Case Study1. In *Strike-Slip Deformation, Basin*

Formation, and Sedimentation (Vol. 37, pp. 0). SEPM Society for Sedimentary Geology. https://doi.org/10.2110/pec.85.37.0211

Shibata, T. (1990). Complex zoning in plagioclase feldspars from ODP site 648. Proceedings of Ocean Drilling Program, Scientific Results.

Suzuki, Y., & Fujii, T. (2010). Effect of syneruptive decompression path on shifting intensity in basaltic sub-Plinian eruption: Implication of microlites in Yufune-2 scoria from Fuji volcano, Japan. *Journal of Volcanology and Geothermal Research*, *198*(1-2), 158-176.

Temel, A., Gundogdu, M. N., & Gourgaud, A. (1998). Petrological and geochemical characteristics of Cenozoic high-Kcalc-alkaline volcanism in Konya, Central Anatolia, Turkey *Journal of Volcanology and Geothermal Research*, *85*(1-4), 327-354.

Tsuchiyama, A. (1985). Dissolution kinetics of plagioclase in the melt of the system diopside-albite-anorthite, and origin of dusty plagioclase in andesites. *Contributions to Mineralogy and Petrology*, *89*(1), 1-16.

Üstündağ, A. (1987). *Sızma-Kurşunlu-Meydan-Bağrıkurt köyleri arasında karadağ çevresinin jeolojisi* [MSc, Selcuk Uni.]. Konya.

Uyanık, C., & Koçak, K. (2016). Geochemical characterıstıcs of the Erenlerdagı volcanics, Konya, Central Turkey. . The 14th International Congress, Thessaloniki, May 2016., Thessaloniki, Greece.

Vernon, R. (1991). Interpretation of microstructures of micro-granitoid enclaves. *Enclaves and granite petrology*, 277-291.

Vernon, R. (2004). Microstructures of deformed rocks. *A practical guide to rock microstructure. Cambridge University Press, Cambridge*, 295-474.

Vernon, R. H. (2010). Granites really are magmatic: Using microstructural evidence to refute some obstinate hypotheses. *The Journal of the Virtual Explorer*, *35*, 1-36.

Wyllie, P. J., Cox, K. G., & Biggar, G. M. (1962). The Habit of Apatite in Synthetic Systems and Igneous Rocks. *Journal of Petrology*, *3*(2), 238-243. https://doi.org/10.1093/petrology/3.2.238